REPORT DOCUMENTATION PAGE

Form Approved
OMB No. 0704-01-0188

PLEASE DO NOT RETURN YOUR FORM TO THE ABOVE ADDRESS.

1. REPORT DATE *(DD-MM-YYYY)*	2. REPORT TYPE	3. DATES COVERED *(From - To)*
15-11-2004	REPRINT	

4. TITLE AND SUBTITLE

Ion-molecule rate constants and branching ratios for the reaction of $N_3^+ + O_2$ from 120 to 1400 K

5a. CONTRACT NUMBER

5b. GRANT NUMBER

5c. PROGRAM ELEMENT NUMBER
61102F

6. AUTHORS
Svetozar Popovic*, Anthony J. Midey, Skip Williams, Abel I. Fernandez, A.A. Viggiano, Peng Zhang**, and K. Morokuma

5d. PROJECT NUMBER
2303

5e. TASK NUMBER
BM

5f. WORK UNIT NUMBER
A1

7. PERFORMING ORGANIZATION NAME(S) AND ADDRESS(ES)

Air Force Research Laboratory /VSBXT
29 Randolph Road
Hanscom AFB, MA 01731-3010

8. PERFORMING ORGANIZATION REPORT NUMBER
AFRL-VS-HA-TR-2005-1189

9. SPONSORING/MONITORING AGENCY NAME(S) AND ADDRESS(ES)

10. SPONSOR/MONITOR'S ACRONYM(S)
AFRL/VSBXT

11. SPONSOR/MONITOR'S REPORT NUMBER(S)

12. DISTRIBUTION/AVAILABILITY STATEMENT
Approved for public release; distribution unlimited.

13. SUPPLEMENTARY NOTES
Reprinted from J. Chem. Phys., Vol. 121, No. 19, pp. 9481-9488. *Dept of Physics, Old Dominion Univ., Norfolk, VA 23529-0116. **Cherry L. Emerson Ctr. for Scientific Computation and Dept of Chemistry, Emory Univ., Atlanta, GA 30322

14. ABSTRACT The kinetics of N_3^+ reacting with O_2 has been studied from 120 to 1400 K using both a selected ion flow tube and high-temperature flowing afterglow. The rate constant decreases from 120 K to ~1200 K, then increases slightly to 1400 K. which compares well to most of the previous measurements in the overlapping temperature range. Comparing the results to drift tube data shows little difference between increasing the translational energy available for reaction and increasing the internal energy of the reactants over much of the range, i.e., all types of energies drive the reactivity equally. The reaction produces both NO^+ and NO_2^+; the latter is shown to be the higher energy NOO^+ linear isomer. The ratio of NOO^+ to NO^+ is over 2 at 120 K, decreasing to less than 0.01 at 1400K because of dissociation of NOO^+ at the higher temperatures. This ratio decreases exponentially with increasing temperature. High-level theoretical calculations have also been performed to complement the data. Calculations using multi-reference configuration interaction theory at the MRCISD(Q)/cc-pVTZ level of theory show that singlet NOO^+ is linear and is 4.5 eV higher in energy than ONO^+. A barrier of 0.9 eV prevents dissociation into NO^+ and $O(^1D)$; however, crossing to a triplet surface connects to NO^+ and $O(^3P)$ products. A singlet and a triplet potential energy surface leading to products have been determined using coupled cluster theory at the CCSD(T)/aug-cc-pVQZ level on structures optimized at the Becke3-Lee, Yang , and Parr (B3LYP)/aug-cc-pVTZ levels.

15. SUBJECT TERMS

Rate constants
High temperature
Ion-molecule
Flowing afterglow

16. SECURITY CLASSIFICATION OF:			17. LIMITATION OF ABSTRACT	18. NUMBER OF PAGES	19a. NAME OF RESPONSIBLE PERSON
a. REPORT	b. ABSTRACT	c. THIS PAGE			A. A. Viggiano
UNCL	UNCL	UNCL	UNL		19B. TELEPHONE NUMBER *(Include area code)* (781) 377-4028

Ion-molecule rate constants and branching ratios for the reaction of $N_3^+ + O_2$ from 120 to 1400 K

Svetozar Popovic,[a] Anthony J. Midey, Skip Williams, Abel I. Fernandez, and A. A. Viggiano[b]
Air Force Research Laboratory, Space Vehicles Directorate, Hanscom Air Force Base, Massachusetts 01731-3010

Peng Zhang and K. Morokuma
Cherry L. Emerson Center for Scientific Computation and Department of Chemistry, Emory University, Atlanta, Georgia 30322

(Received 7 July 2004; accepted 25 August 2004)

The kinetics of the reaction of N_3^+ with O_2 has been studied from 120 to 1400 K using both a selected ion flow tube and high-temperature flowing afterglow. The rate constant decreases from 120 K to ~1200 K and then increases slightly up to the maximum temperature studied, 1400 K. The rate constant compares well to most of the previous measurements in the overlapping temperature range. Comparing the results to drift tube data shows that there is not a large difference between increasing the translational energy available for reaction and increasing the internal energy of the reactants over much of the range, i.e., all types of energies drive the reactivity equally. The reaction produces both NO^+ and NO_2^+, the latter of which is shown to be the higher energy NOO^+ linear isomer. The ratio of NOO^+ to NO^+ decreases from a value of over 2 at 120 K to less than 0.01 at 1400 K because of dissociation of NOO^+ at the higher temperatures. This ratio decreases exponentially with increasing temperature. High-level theoretical calculations have also been performed to compliment the data. Calculations using multi-reference configuration interaction theory at the MRCISD(Q)/cc-pVTZ level of theory show that singlet NOO^+ is linear and is 4.5 eV higher in energy than ONO^+. A barrier of 0.9 eV prevents dissociation into NO^+ and $O(^1D)$; however, a crossing to a triplet surface connects to NO^+ and $O(^3P)$ products. A singlet and a triplet potential energy surface leading to products have been determined using coupled cluster theory at the CCSD(T)/aug-cc-pVQZ level on structures optimized at the Becke3-Lee, Yang, and Parr (B3LYP)/aug-cc-pVTZ level of theory. The experimental results and reaction mechanism are evaluated using these surfaces. © *2004 American Institute of Physics.* [DOI: 10.1063/1.1807376]

I. INTRODUCTION

Air plasmas at elevated pressures are currently the subject of intensive study for a variety of applications. Typical nonequilibrium plasmas have heavy particle temperatures below 1000 K and average electron energies on the order of a few eV. These conditions are favorable for associative ionization processes and the presence of polyatomic nitrogen ions such as N_3^+ and N_4^+ is expected. However, temperature dependent data even for the relatively simple cases involving reactions of these ions with major species are insufficient or nonexistent.

In light of these issues, the kinetics of the reaction of N_3^+ with O_2 has been studied in more detail. The reaction has two observed product channels:

$$N_3^+ + O_2 \rightarrow NO^+ + (N_2O) + 466 \text{ kJ mol}^{-1} \quad (1a)$$

$$\rightarrow NO_2^+ + N_2 + 124 \text{ kJ mol}^{-1}, \quad (1b)$$

where the N_2O product may be dissociated, i.e., N_2+O, reducing the exothermicity of the reaction to 299 kJ mol^{-1}, or production of N+NO, which would make the reaction endothermic by 14 kJ mol^{-1}. The heat of formation of N_3^+ has been obtained by combining the average of the experimental heats of formation of N_3 from the work of Continetti *et al.*[1] and Martin *et al.*[2] with the ionization potential from the work of Dyke *et al.*,[3] which are in good agreement with the recent theoretical values of Dixon *et al.*[4] For the NO_2^+ thermochemistry, we use the present *ab initio* calculations for the NOO^+ isomer (see below). All of the other values are from the NIST Webbook.[5] Note also that the NIST Webbook recommended value for the heat of formation of N_3 is 52 kJ mol^{-1} lower than the values used here.

In a flowing afterglow, Dunkin *et al.*[6] measured the first experimental value for the total rate constant for reaction (1) at 200 K and obtained a value of $k=1\times10^{-10}$ cm^3 s^{-1}. Smith *et al.*[7] have determined a rate constant of 5.1×10^{-11} cm^3 s^{-1} for the reaction at 300 K in a selected ion flow tube (SIFT), which is an order of magnitude less than the Langevin collision rate constant of 7.0×10^{-10} cm^3 s^{-1}. In addition, Lindinger[8] has measured the rate constants for the N_3^+ reaction with O_2 in a flow drift tube (FDT) at 298 K

[a]Permanent address: Department of Physics, Old Dominion University, Norfolk, VA 23529-0116.
[b]Author to whom correspondence should be addressed; Electronic mail: albert.viggiano@hanscom.af.mil

over a wide range of center-of-mass kinetic energies at low pressures. A rate constant of 6×10^{-11} cm^3 s^{-1} has been reported by Lindinger at zero field (0.038 eV), which decreases to a minimum at 0.25 eV kinetic energy and then increases at higher kinetic energy. The rate constant has been observed to be independent of pressure over the limited pressure range 0.139–0.253 Torr studied. Hiraoka[9] measured the rate constant for reaction (1) from 64 to 552 K using a high pressure mass spectrometer (HPMS) at ca. 3 Torr and found that the rate constant decreases monotonically with increasing temperature over the entire temperature range. Matsuoka *et al.*[10] have also found a total reaction rate constant at 294 K for reaction (1) of 7.1×10^{-11} cm^3 s^{-1} using a time-resolved atmospheric pressure ionization mass spectrometer (TRAPI).[10] There is good agreement among the room temperature thermal rate constants reported by Smith *et al.*, Lindinger, and Matsuoka *et al.*

Product formation has also been studied. Smith *et al.* have determined that the product ions formed in reaction (1) are 70% NO^+ and 30% NO_2^+ at 300 K.[7] By contrast, the drift tube results of McCrumb and Warneck[11] and the TRAPI measurements of Matsuoka *et al.*[12] indicate that the majority product is NO_2^+. Dunkin *et al.*[6] suggest that an additional "switching" reaction channel results in a third product channel giving O_2^+, proceeding through an intermediate excited state of a $(N^+\cdot O_2)^*$ complex that can decay into $NO^+ + O$ and $O_2^+ + N$ products, or can be stabilized collisionally or radiatively to form NO_2^+. Matsuoka *et al.*[10] have also reported that the NO_2^+ ions formed are rapidly lost in collisions with N_2 at atmospheric pressure with an effective decay constant of 3.0×10^4 s^{-1}, carefully ruling out any interfering reactions of NO_2^+. Hiraoka[9] measured the relative branching ratios of the NO_2^+ and NO^+ products from 64 to 552 K and found that $[NO_2^+]/[NO^+]$ decreases monotonically with increasing temperature which is in general agreement with the values of Matsuoka *et al.* from 303 to 384 K.[12]

Matsuoka *et al.*[12] further addressed the problem of thermal stability of the NO_2^+ product of reaction (1). They determined that the decay of NO_2^+ into NO^+ has a strong temperature dependence, increasing exponentially with increasing temperature. Furthermore, they have found that NO_2^+ from reaction (1) is reactive and thermally dissociates, while the NO_2^+ formed in the reaction of O_2^+ with NO_2 is thermally stable and unreactive. Therefore, they conclude that the two NO_2^+ ions do not have the same structure. These authors further argue that the atomic arrangement in the NO_2^+ from reaction (1) should be the higher energy NOO^+ linear isomer.[12]

However, the HPMS measurements of Hiraoka indicate that ONO^+ is the isomer formed by reaction (1), based on the lack of thermal unimolecular dissociation of NO_2^+ at 465.7 K and *ab initio* calculations of the successive binding energies of N_2 ligands in $NO_2^+(N_2)_n$ clusters containing ONO^+. The calculated energies agree with the measured values, whereas the preliminary calculations of Hiraoka and Yamabe show that NOO^+ is highly unstable.[13] Differences in the nucleophilic properties of N_2 vs O_2 further imply that the observed product is ONO^+.[9]

In order to elucidate the kinetics of the $N_3^+ + O_2$ system, the rate constants and product ion branching ratios for reaction (1) were measured from 120 to 1400 K using two complementary instruments. The discrepancy concerning the NO_2^+ product isomer was investigated by experimental and theoretical analyses of the thermal stability, reactivity, energetics, and structure of the various isomeric forms of NO_2^+ (including barriers to rearrangement). The combination of a SIFT and high-temperature flowing afterglow (HTFA) allows this wide temperature range to be probed. Comparing the current rate constants to the previous measurements as a function of temperature[9] and kinetic energy[8] shows the effects of different types of energies on the reactivity. A potential energy profile has been calculated to elucidate the reaction mechanism.

II. EXPERIMENT/COMPUTATION

A. Kinetics measurements

An experimental study of the $N_3^+ + O_2$ reaction was performed using two separate techniques in order to encompass the temperature range from 120 to 1400 K. The SIFT has been used in the temperature range between 120 and 500 K, while the HTFA measurements have spanned the 350–1400 K range. Details of the two systems are described elsewhere.[14–16] All of the reagent gases have been used without further purification.

In the SIFT, N_3^+ ions are generated from N_2 in an effusive source in a high-pressure source region. High purity molecular nitrogen is taken from the boil-off of a high-pressure liquid nitrogen dewar. Two mechanisms for N_3^+ generation are operative: three-body association of N^+ with N_2 and Penning ionization of N_2, the latter of which is shown in Eq. (2),

$$N_2^* + N_2 \rightarrow N_3^+ + N. \tag{2}$$

Mass selection of N_3^+ using a quadrupole mass filter before injection into the fast flow of He buffer gas (AGA, 99.995%) produces N_3^+ in the flow tube in >99% purity. After reaction, the ions are sampled through a blunt nose cone aperture and are analyzed by a quadrupole mass analyzer, and then detected by an electron multiplier. Rate constant measurements are performed at two reaction distances, 36 and 52 cm, and the data do not vary between the two reaction lengths within the experimental uncertainty. Measurement of the exponential decay of the primary ion signal as a function of the O_2 concentration (Massachusetts Oxygen, 99.999%) under pseudo-first-order conditions, coupled with the previously measured ion velocities, yields the rate constant. The average relative error in the rate constants is ±15% with absolute errors of ±25%.[15]

The product ion branching ratios are determined in the SIFT by measuring the relative magnitude of the NO_2^+ and NO^+ signals obtained from extrapolating to zero O_2 concentration:

$$\%[NO_2^+] = 100\times[NO_2^+]/([NO_2^+]+[NO^+]). \tag{3}$$

In addition, the ratio of NO_2^+ to NO^+, r, is obtained as shown in Eq. (4),

$$r = \%[NO_2^+]/(100 - \%[NO_2^+]). \quad (4)$$

This ratio has been measured over a relatively high range of oxygen concentrations, approaching 0.2% of the total gas flow. No secondary chemistry is observed and the percentage of NO_2^+ is independent of O_2 flow. The relative uncertainty of the branching ratios is ±10% of the major product peaks.[17]

In the HTFA, the ions are generated in an ion source region positioned orthogonal to the quartz reaction tube.[14] The source has a 0.5 in. diameter exit aperture for these experiments, so that the source pressure is higher than that found in the flow tube. Nitrogen is introduced downstream from a thoriated iridium filament biased to 100–150 V with 0.1–4 mA emission current. The same two reaction processes generate N_3^+ ions as in the SIFT. A helium buffer flow up to 30 000 SCCM is introduced through the source region and carries the ions into the flow tube where a commercial furnace controls the temperature (SCCM denotes cubic centimeter per minute at STP). Typical operating pressures in the flow tube are between 0.8 and 1.5 Torr. O_2 is added 52.7 cm upstream from the nose cone sampling plate in the region where the ions have reached thermal equilibrium. A small fraction of the flow is again sampled and the ions are analyzed by a quadrupole mass analyzer, and then detected by an electron multiplier. The N_3^+ ion decay rate does not change with the N_2 source gas flow at rates of 125–500 SCCM, indicating that the production of the ions is complete before the reactant inlet. Residual water contaminant in the helium buffer is reduced using a liquid nitrogen cooled sieve trap.

At higher temperatures, alkali ions thermionically emitted from the quartz flow tube are inevitable, but these ions are nonreactive background species in the mass spectrum. Invariance of the alkali ion signal as a function of O_2 flow has been used as an indicator that the flow tube chemistry has properly equilibrated as demonstrated previously.[18] At 1400 K, the level of the $^{41}K^+$ signal was comparable to the level of the N_3^+ signal ($m/z = 42$), and the mass resolution of the quadrupole filter was adjusted so that the two mass peaks are separated. Average relative errors of the N_3^+ decay rate are ±12% with absolute errors of ±25%.[16]

Unfortunately, a pure N_3^+ signal is not possible in the HTFA because of the lack of upstream mass selection and the mechanism for N_3^+ ion generation. Due to the complexity of the reactions involving N^+, N_2^+, N_3^+, N_4^+, and NO^+ also present in the flow tube, it is impossible to determine the branching ratios for the two reaction channels by simultaneously following the two products, especially since NO^+ is also a product of a number of background reactions, e.g., $N^+ + O_2$. Fortunately, none of the contaminant ions react with O_2 to produce an ion at $m/z = 46$, the mass of NO_2^+. Therefore, the NO_2^+ fraction at a given concentration of oxygen has been evaluated in the HTFA from Eq. (5) below,

$$\%[NO_2^+] = 100([NO_2^+] - [NO_2^+]_0)/([N_3^+]_0 - [N_3^+]), \quad (5)$$

where the differences between the ion signals at a given O_2 concentration and zero O_2 concentration are used. The relative uncertainty in the product distributions determined this way is also 10%. This uncertainty is determined from the agreement with the SIFT results shown below.

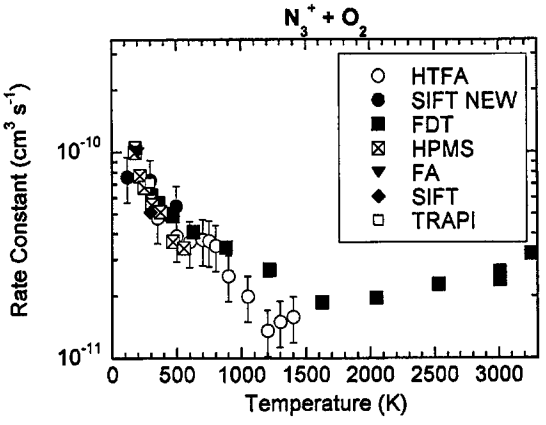

FIG. 1. Temperature dependence of the rate constants for the reaction of N_3^+ with O_2 as recently measured in the selected ion flow tube (SIFT) and high-temperature flowing afterglow (HTFA). Also included are measurements performed with a flow drift tube (Ref. 8), TRAPI (Ref. 10), SIFT (Ref. 7), flowing afterglow (FA) (Ref. 6), and HPMS (Ref. 9). The Langevin collision rate constant for this reaction is $7.0 \times 10^{-11}\ cm^3\ s^{-1}$.

B. *Ab initio* calculations

Energies of the various isomers of the NO_2^+ species on the ground state singlet potential energy surface have been calculated at different levels of theory. Here we present only the energetics of the NOO^+ isomer optimized using multireference configuration interaction at the MRCISD(Q)(15e,12o)/cc-pVTZ level. The detailed theoretical results will be presented in a separate paper.

A potential energy profile has also been calculated. Geometries were optimized using density functional theory (DFT) at the Becke3-Lee, Yang, and Parr (B3LYP)/aug-cc-pVTZ level, where aug-cc-pVTZ denotes Dunning's correlation consistent polarized valence triple-zeta basis set augmented with diffuse functions.[19] Frequency calculations have been performed at the same level as the geometry optimization to determine whether the species are stable molecules or transition states. Intrinsic reaction coordinate (IRC) calculations have been carried out to confirm the connectivity of every optimized transition state at the same level. To obtain better energetics, single point energy calculations using coupled cluster theory at the CCSD(T)/aug-cc-pVQZ level have been performed on the B3LYP/aug-cc-pVTZ optimized geometries, where aug-cc-pVQZ denotes Dunning's correlation consistent polarized valence quadruple zeta basis set augmented with diffuse functions.[19]

III. RESULTS AND DISCUSSION

A. Rate constants

Figure 1 shows the rate constants of the $N_3^+ + O_2$ reaction as a function of temperature as measured in the SIFT and HTFA covering the 120–1400 K range; error bars denote our ±15% experimental uncertainty. The rate constants decrease substantially with temperature up to 1200 K, reaching

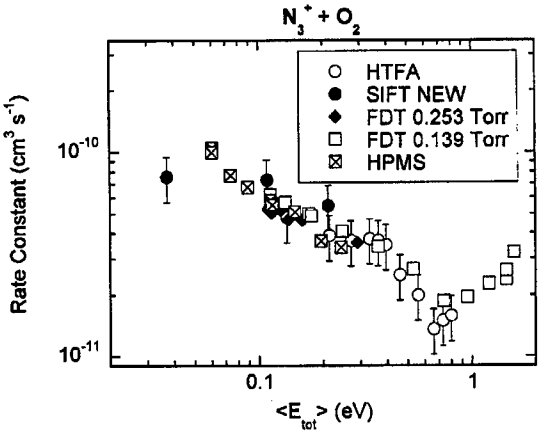

FIG. 2. Dependence of the rate constants for the reaction of N_3^+ with O_2 on the sum of the average total energy (translational, rotational, and vibrational) for the present data and those obtained in the FDT experiment (Ref. 8).

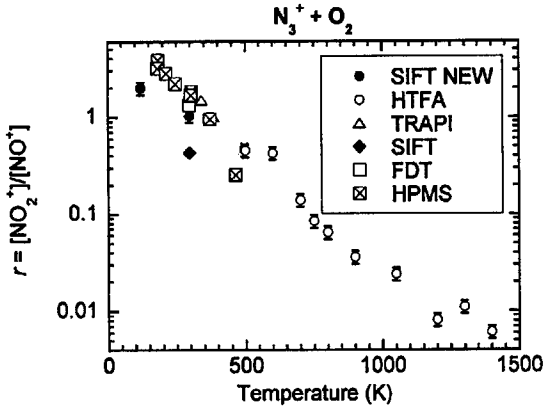

FIG. 3. Temperature dependence of the product ion distribution in the reaction of N_3^+ with O_2. The TRAPI results are from the work of Matsuoka *et al.* (Ref. 12) and the previous SIFT results are from the work of Smith *et al.* (Ref. 7). DT results are from the work of McCrumb and Warneck (Ref. 11) and the HPMS from the work of Hiraoka (Ref. 9).

a minimum at this temperature and then increase up to 1400 K. Data from the two instruments, the SIFT and the HTFA, agree in the overlapping temperature region within the experimental uncertainty.

Measurements from the other temperature dependent experiments[6,7,9,10] discussed in the Introduction are also shown in Fig. 1 and agree well with the present work, if the rate constants measured below ~180 K in the HPMS are excluded. The previous flow drift tube results are discussed separately below. These values are not shown because clusters of the type $N_3^+(N_2)_n$ are formed and because the rate constants do not correspond purely to N_3^+ as the reactant ion. Below 180 K, the HPMS rate constants show a steeper increase with decreasing temperature, indicating that the $N_3^+(N_2)_n$ ions react faster than does bare N_3^+.[9] This interference is not a problem in the current experiments because no N_2 is present in the flow tube of the SIFT and clustering to N_3^+ does not occur at high temperature in the HTFA. The room temperature value measured by Matsuoka *et al.* at atmospheric pressure is slightly larger than the rest of the measurements and may have been slightly influenced by clustering.[10] However, the atmospheric pressure value does agree within the experimental error. All of the rate constants shown are considerably smaller than the Langevin collision rate constant of $7.0\times10^{-10}\,cm^3\,s^{-1}$.

Also shown in Fig. 1 are rate constants from a flow drift tube experiment (FDT) taken as a function of center-of-mass kinetic energy.[8] The kinetic energy is converted to a translational temperature by $\langle KE_{c.m.}\rangle = 3/2kT_{eff}$. The agreement with the drift tube data is good at low temperature, but at temperatures around 800 K and higher, the data diverge for reasons to be discussed below. In addition, the current results suggest that the rate constants begin to increase after reaching a minimum at a translational temperature lower than that found in the drift tube.[8]

In order to compare the role of various types of energies, the data are replotted as a function of average total energy in Fig. 2. The rotational and vibrational temperatures of the reactant ions in the FDT experiments are determined from the center-of-mass collision energy for ion-buffer gas collisions ($\langle KE_{buffer}\rangle = 3/2kT_{rot}$).[20] Note that a N_2 buffer was used in the drift tube experiments. The average vibrational energy is calculated as an ensemble average over a Boltzmann distribution of harmonic vibrational frequencies of the reactants.[5] At low temperatures, N_3^+ vibrations predominantly contribute, while the O_2 vibrations contribute only at temperatures over about 1000 K.[5]

The rate constants from all of the data sets decrease with increasing energy and reach a small plateau in the 0.2–0.4 eV range before decreasing again to a minimum at 0.7 eV. Above this energy, the rate constants increase with increasing energy. The temperature and kinetic energy data are indistinguishable, indicating that all forms of energy that are excited in this range control reactivity approximately the same. Of course, cancellation of effects is possible, but past experience indicates this occurrence is unlikely.[21] The equivalency of translational and rotational energies is a typical behavior for most ion-molecule reactions. Vibrational excitation often has a different effect than the other forms of energy.[21]

B. Branching ratios

Previous results on the branching ratios for reaction (1) are few in number and contradictory. A SIFT experiment by Smith *et al.* yields a value of $r=[NO_2^+]/[NO^+]=0.43$ at 300 K.[7] However, a preference for reaction channel (1b) ($r=1.33$) was observed in the drift tube measurement by McCrumb and Warneck at the same temperature.[11] Matsuoka *et al.* reported that r decreases from $r=1.72$ at 303 K to $r=1$ at 384 K in a TRAPI experiment, which suggests that reaction (1b) is preferred at lower temperatures and that this preference may be reversed at higher temperatures, i.e., $r<1$.[12] Thus, the results from an earlier SIFT experiment[7] are the opposite of the results from the drift tube[11] and the TRAPI experiment.[12] The present work attempts to (a) address the discrepancy in the value of r, (b) verify its temperature dependence, and (c) elucidate the nature of the NO_2^+ product.

Branching ratios as a function of temperature obtained from the current experiments are shown in Fig. 3, given as

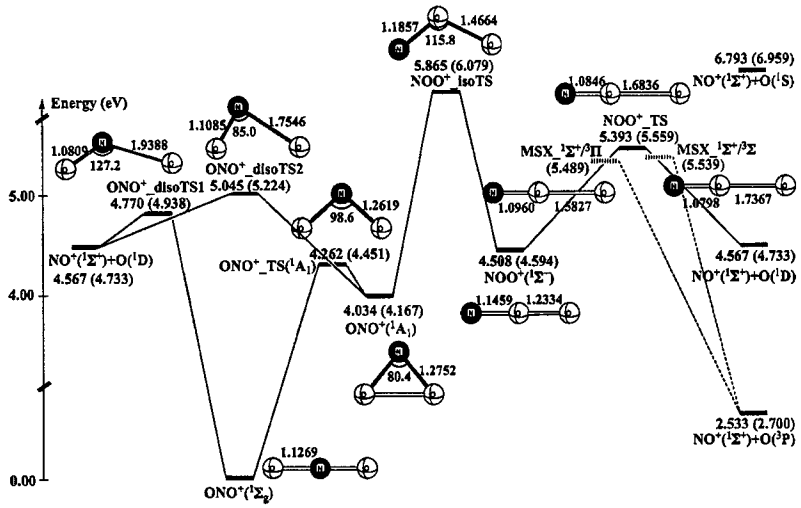

FIG. 4. Potential energy profile of the NO_2^+ singlet isomers optimized at the MRCISD(Q)/cc-pVTZ level of theory. On the structures, numbers are bond distances and angles (in angstrom and degree). For the energetics, plain numbers are with zero-point energy (ZPE) correction, and numbers in the parentheses are without ZPE correction. Only ONO+_disTS2 was calculated at the MRCISD(Q)/cc-pVTZ//CASSCF/cc-pVTZ level.

the ratio r defined in Eq. (4). The most striking feature of the present results is a monotonic exponential decrease of r with increasing temperature over several orders of magnitude, i.e., a substantial decrease in the amount NO_2^+ observed for reaction (1) at high temperature. This downward trend is in excellent agreement with the HPMS temperature dependent data up to ca. 450 K, indicating that the crossover to $r<1$ predicted by Matsuoka[12] does occur. The present data further indicate that the trend continues until the highest temperatures. There are no obvious explanations for (a) the exponential nature of the decline and (b) for the disagreement of the highest temperature HPMS point.

The other anomalous point on the branching ratio plot is from the earlier SIFT study.[7] In contrast to the present study where N_3^+ is injected cleanly into a helium buffer, the previous SIFT value was obtained by injecting N^+ into a mixed He (0.45 Torr)/N_2 (0.2 Torr) buffer and letting N^+ cluster with N_2 to form N_3^+. A potential problem would occur if some N^+ had survived into the reaction zone (but not necessarily to the mass spectrometer) since the reaction of N^+ with O_2 produces NO^+ but not NO_2^+.[22] In addition, Matsuoka *et al.*[10] have shown that the NO_2^+ formed in reaction (1) subsequently reacts with N_2 with a rate constant of 1.2×10^{-15} cm^3 s^{-1} to form NO^+. This reaction would partially convert NO_2^+ to NO^+ in the previous SIFT experiment and skew the branching ratio to a value less than 1.

C. NO_2^+ structures and unimolecular reactions

The structure of the NO_2^+ ions produced in reaction (1) has also been the subject of debate. Matsuoka and co-workers[10,12] have reported that the NO_2^+ ions formed by reaction (1b) in the TRAPI are lost in collisions with N_2 at atmospheric pressure with an effective decay constant of 3.0×10^4 s^{-1} or a bimolecular rate constant of $\sim3\times10^{-16}$ cm^3 s^{-1}. Furthermore, they observed that this decay (a) produces NO^+, (b) is independent of the O_2 and N_2 content in their reaction gas mixture, and (c) is temperature dependent. In their earlier paper,[10] they assigned the reactivity to

$$NO_2^+ + N_2 \rightarrow NO^+ + N_2O \qquad (6)$$

with a bimolecular rate of 1.2×10^{-15} cm^3 s^{-1}. In their subsequent paper, they attribute the loss of NO_2^+ to thermal decomposition of an isomer having a NOO^+ structure, mainly because the rate did not change with buffer gas density. The observed decay rate of NO_2^+ measured over a relatively narrow range between 294 and 384 K using TRAPI increases exponentially with increasing temperature, giving a rate of $(5.6\times10^7)\exp(-4500/RT)$ s^{-1}. Furthermore, they have found that NO_2^+ from reaction (1) reacts strongly with C_2H_6 to form $C_2H_5^+$. However, the NO_2^+ formed in the reaction of O_2^+ with NO_2 does not react with C_2H_6. Therefore, they concluded that the two NO_2^+ ions do not have the same structure, also supporting the thermal decomposition hypothesis.

In contrast, the HPMS measurements of Hiraoka indicate that ONO^+ is the isomer formed.[9] Loss of NO_2^+ is not observed at 465.7 K in the HPMS. *Ab initio* calculations of the successive binding energies of N_2 ligands in $NO_2^+(N_2)$ clusters with ONO^+ agree with the measured values, whereas their preliminary calculations show that NOO^+ is highly unstable.[13] In the experiments of Matsuoka *et al.* at atmospheric pressure,[10,12] the single exponential decay of the NO_2^+ signal indicates that only one isomer is formed.

To address this issue, both high-level theoretical calculations and an experimental test of the reactivity of the NO_2^+ produced in reaction (1) have been performed. The details of the calculations are presented in a separate paper, with only the most relevant results at the highest level of calculation, MRCISD(Q)/cc-pVTZ, presented here in Fig. 4. The calculations show that the NOO^+ isomer is stable, with an energy of 4.51 eV above the ground state linear ONO^+ isomer. The $NOO^+(^1\Sigma^+)$ isomer is linear with a N–O bond distance of 1.146 Å and an O–O bond distance of 1.233 Å. A barrier of 0.89 eV prevents the isomer from dissociating to $NO^+(^1\Sigma^+)+O(^1D)$, which is only 0.060 eV endothermic. Production of $NO^+(^1\Sigma^+)$ and $O(^3P)$ from $NOO^+(^1\Sigma^+)$ is exothermic by almost 2 eV, correlating to three triplet surfaces accessed by curve crossings. Two minima of the singlet-triplet seam-of-crossing (MSX) have been located: MSX_$^1\Sigma^+/^3\Pi$ ca. 0.07 eV below NOO^+_TS and MSX_$^1\Sigma^+/^3\Sigma$ ca. 0.02 eV below NOO^+_TS, as shown in Fig. 4. Spin-orbit calculations indicate that both of them have

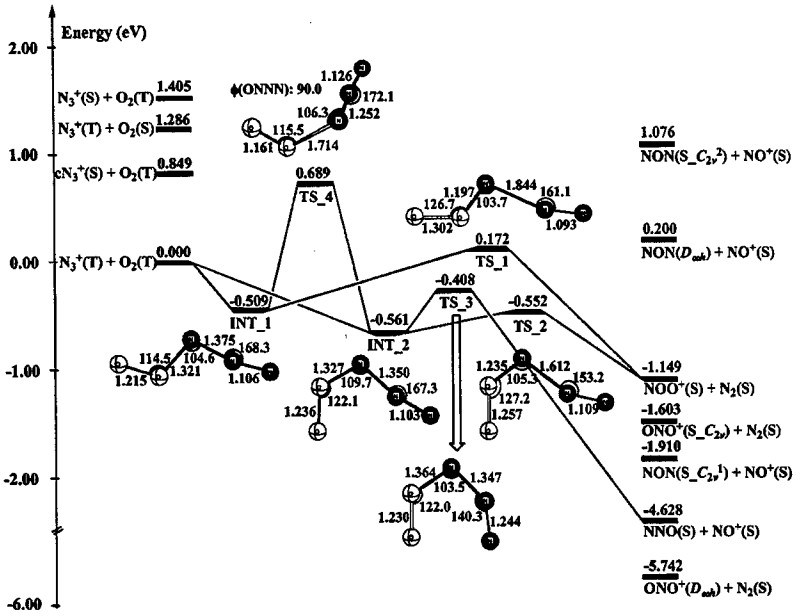

FIG. 5. Singlet potential energy surface for the reaction of $N_3^+ + O_2$ calculated at the CCSD(T)/aug-cc-pVQZ//B3LYP/aug-cc-pVTZ level of theory. On the structures, numbers are bond distances and angles (in angstrom and degree). For the energetics, ZPE correction has been applied.

very strong interactions: 65.5 cm^{-1} for each of the $^3\Pi$ components with $^1\Sigma^+$ and 35.7 cm^{-1} for the MSX_$^1\Sigma^+/^3\Sigma$, suggesting that predissociation could easily occur. On the singlet ground state, there is also a bent ($^1A_1$) isomer of ONO^+ with an ∠ONO of 80°. This bent form lies 4.03 eV above the most stable linear ONO^+, and a small barrier of 0.23 eV relative to the bent isomer links them. This barrier is relatively small and thermal isomerization in the presence of buffer gas should be fast enough to prevent this species from being observed in our apparatus.[23] However, the barrier between linear NOO^+ and bent ONO^+ isomers, NOO^+_isoTS, is found to be quite large, 1.36 eV from the linear NOO^+ isomer. The dissociation processes of ONO^+ isomers are also investigated. Two corresponding transition states, ONO^+_disTS1 and ONO^+_disTS2, connecting the linear and bent isomers are found to be 4.77 and 1.01 eV above the corresponding isomers, respectively. Note that the activation energy found by Matsuoka *et al.*[10,12] for NO_2^+ reacting with N_2 is much smaller than the barrier found here for dissociation to NO^+, indicating that the process observed is probably not thermal dissociation. (Note also that using the new energetics for N_3, the production of $N_2 + O(^1D) + NO^+$ is 0.99 eV exothermic.) Therefore, all of the transition states and isomers except the NOO^+_isoTS discussed above lie below the entrance channel energy for $N_3^+ + O_2$ at 300 K as shown in Fig. 4.

It is relatively easy to determine if a high energy form of NO_2^+ is generated in the present experiments. A sufficiently large amount of O_2 can be added upstream in the flow tube of the SIFT to drive reaction (1) to completion before a second gas is added downstream to test the chemistry of the product ions. What is required is a gas that does not react with the ground state ONO^+ isomer, but will react with the NOO^+ isomer (assuming that the bent ONO^+ species, if formed, thermally isomerizes to the linear ground state). Xenon is a good candidate since it is a generally unreactive gas. For this test, Xe (Air Products, 99.995%) is introduced into the SIFT at a distance 30 cm downstream from the O_2 inlet. In a separate experiment for comparison purposes, ground state ONO^+ is generated in the source region of the SIFT by electron impact on nitrogen dioxide (Matheson, 99.5%). These ONO^+ ions are mass-selected and then reacted with Xe in the normal manner. NO_2^+ injected into the flow tube from the ionization of nitrogen dioxide in the source does not react with Xe. By contrast, the 46 amu ion generated by reaction (1) is totally consumed when Xe is added to the SIFT. The reaction turns out to be more complicated than expected, giving two products:

$$NOO^+ + Xe \rightarrow NO^+ + (Xe + O) + 356 \text{ kJ mol}^{-1} \quad (6a)$$

$$\rightarrow XeO^+ + NO + 108 \text{ kJ mol}^{-1}. \quad (6b)$$

The bulk of the reaction produces NO^+. However, the reaction is sufficiently exothermic so that the neutral product could be either XeO or Xe+O. This difference in reactivity confirms that the NO_2^+ made in reaction (1) is a high-energy isomer and is not in the linear ONO^+ form, in agreement with the TRAPI results.[12] Production of XeO^+ is rare, but it has been observed previously.[24] We have also confirmed that C_2H_6 reacts with NOO^+ from reaction (1) to produce $C_2H_5^+$ and that linear ONO^+ does not.

D. Potential energy surface and reaction mechanism

Lindinger suggests that the decrease of the rate constant with kinetic energy (or temperature) is due to the lifetime of the complex intermediate decreasing with the increasing relative velocity of the reactants.[8] This assumes that product formation is slow compared to that for dissociation into reactants and that no barrier is above the energy of the reactants. This assertion is probably qualitatively correct but somewhat simplistic for a quantitative description. The increase at higher temperatures/energies is probably attributable to a new mechanism that becomes available.

In order to elucidate the probable mechanisms, CCSD(T) calculations of the potential energy profile have been made as mentioned in the Experiment/Computation. The resulting

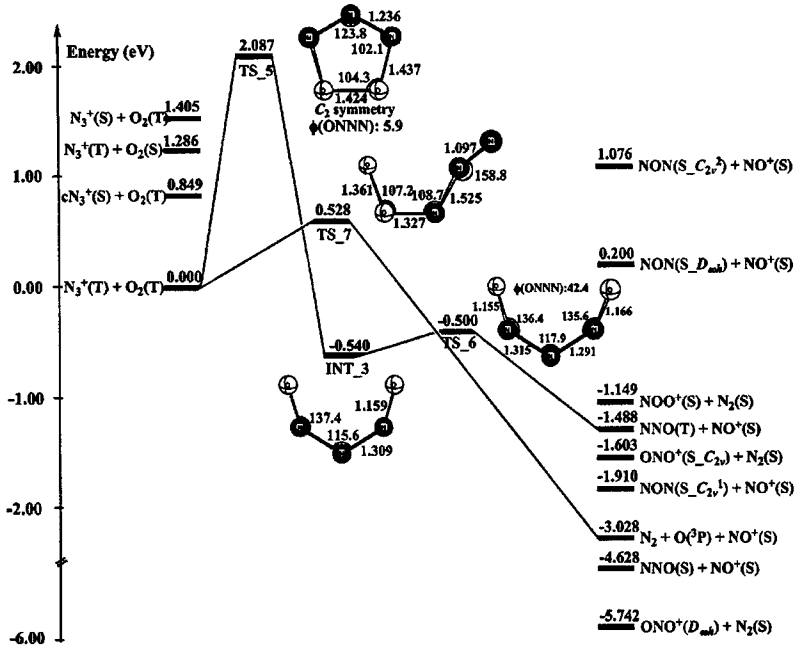

FIG. 6. Triplet potential energy surface for the reaction of $N_3^+ + O_2$ calculated at the CCSD(T)/aug-cc-pVQZ//B3LYP/aug-cc-pVTZ level of theory. On the structures, numbers are bond distances and angles (in angstroms and degree). For the energetics, ZPE correction has been applied.

singlet and triplet potential surfaces are shown in Figs. 5 and 6, respectively. The reactants are triplets and correlate to singlet and triplet products. The connectivity of the transition states has also been confirmed as discussed in the Experiment/Computation.

On the singlet surface shown in Fig. 5, two intermediates are formed directly from the reactants. The first intermediate (INT_1) has the O_2 axis nearly parallel to the quasilinear N_3^+ ($\angle$N–N–N=168°) axis, with $\angle$N–N–O=105° and $\angle$N–O–O=115°. This "*trans*" structure lies 0.51 eV below the energy of the reactants. The other "*cis*" intermediate (INT_2) is more v shaped and lies 0.56 eV below the reactants. A transition state (TS_4) separates the two intermediates and is 1.20 eV above INT_1. INT_1 correlates only to the NOO^+ product, but the reaction must pass through TS_1 with a barrier 0.17 eV above the reactants. Therefore, it is not important at low energies or temperatures. INT_2 is connected to both NO^+ and NOO^+ through separate transition states (TS_3 and TS_2) that are 0.15 and 0.01 eV, respectively, above the energy of INT_2.

On the triplet surface shown in Fig. 6, a V-shaped intermediate (INT_3) is 0.54 eV below the reactants and connects to NO^+ and N_2O singlet products through transition state (TS_6) only 0.04 eV above INT_3. However, INT_3 can only be reached through a cyclic $N_3O_2^+$ transition state complex (TS_5) that is 2.09 eV higher in energy. Another transition state (TS_7) lies 0.53 eV above the reactants and simultaneously produces three fragments: $NO^+(^1\Sigma^+)$, N_2, and $O(^3P)$.

The features of the surfaces illustrated in Figs. 5 and 6 at least qualitatively explain the reactivity. At low temperatures, the reaction occurs at an appreciable fraction of the collision rate and decreases with increasing energy and temperature. That trend is typical for ion-molecule reactions involving surfaces with stable intermediates followed by barriers to reaction. The simplest explanation is that decay of the intermediates into reactants involves a loose transition state and into products involves a tight one. This picture is a more complete description of the mechanism than proposed by Lindinger.

At low energies, reaction (1) occurs on the singlet surface in Fig. 5. Once INT_2 forms, it can decay back into reactants or into either product channel, NOO^+ or NO^+. NOO^+ has the lower barrier and is thus favored at low energy. However, the barrier to NO^+ production is not much higher and the data show that NO^+ is favored by 400 K. Any molecules that form intermediate INT_1 must dissociate back to reactants unless there is enough energy to overcome the barrier. However, sufficient energy is not available until ~800 K (~0.7 eV).

The upturn in the rate constants occurs at a total energy of ~0.7 eV, Fig. 2. Two reaction paths may contribute to this trend at higher energies. First, TS_4 on the single surface connecting the two intermediates INT_1 and INT_2 has a barrier of 0.69 eV, approximately coinciding with the energy at the upturn. Therefore, this additional mechanism leading to products may begin to contribute to the overall reactivity above 0.7 eV, causing an increase in the total rate constant. Second, reaction also becomes possible on the triplet surface in Fig. 6 where the 0.54 eV barrier to TS_7 can be overcome, opening up the channel that produces three fragments including NO^+. In addition, a further reduction in the NOO^+ product at higher energies can come from unimolecular decomposition of NOO^+ giving NO^+. The multireference configuration interaction calculation results shown in Fig. 4 indicate that a crossing from the singlet NOO^+ surface to a triplet surface at MSX_$^1\Sigma^+/^3\Pi$ occurs about 0.8 eV above NOO^+ minimum that allows predissociation to $NO^+(^1\Sigma^+) + O(^3P)$ that is 2 eV lower in energy. This pathway is consistent with the NOO^+ unimolecular decomposition results of Guilhaus *et al.* showing that NOO^+ dissociation produces NO^+ fragments with 2 eV kinetic energy.[25] The present calculations also indicate that a barrier of 0.89 eV exists to dissociate NOO^+ into NO^+ and $O(^1D)$. Since the products

can be formed hot (1.1 eV exothermic), decomposition can happen at relatively lower temperatures, in addition to the mechanisms just discussed.

IV. CONCLUSIONS

The kinetics of the reaction of N_3^+ with O_2 has been studied over a wide temperature range, up to 1400 K. The rate constants are found to decrease from 120 to 1200 K before increasing up to 1400 K and agree with previous measurements taken over limited temperature ranges. Comparing the rate constants to those obtained in a drift tube shows that all forms of energy behave similarly.

Two products are observed, namely, NO_2^+ and NO^+. The former is favored at low temperature and the latter at higher temperature. The ratio r of NO_2^+ to NO^+ decreases exponentially with temperature from $r=2$ at 120 K to $r<0.01$ at 1400 K. In this paper, a straightforward test of the reactivity on the NO_2^+ product ion was made that shows conclusively that this product is a high energy isomer, most likely NOO^+. Theoretical calculations confirm that this is a stable isomer, with a barrier to dissociation of about 0.9 eV. The energy of the NOO^+ isomer is determined to be 4.5 eV above that of the most stable isomer, linear ONO^+. The calculated potential energy surfaces for the reaction giving singlet products explain most of the current data.

ACKNOWLEDGMENTS

The authors thank the Air Force Office of Scientific Research (AFOSR) for its continued support of this laboratory. A.J.M. is under contract (Grant No. F19628-99-C-0069) to Visidyne, Inc., Burlington, MA. A.I.F. acknowledges support under the NRC Research Associate program. S.P. also acknowledges support under the NRC Summer Faculty Program. The work done at Emory University was supported in part by a grant from AFOSR (Grant No. FA9550-04-1-0080). A part of the computer time was made available by a grant from AFOSR under the DoD High Performance Computing Program.

[1] R. E. Continetti, D. R. Cyr, D. L. Osborn, D. J. Leahy, and D. M. Neumark, J. Chem. Phys. **99**, 2616 (1993).
[2] J. M. L. Martin, J. P. Francois, and R. Gijbels, J. Chem. Phys. **93**, 4485 (1990).
[3] J. M. Dyke, N. B. H. Jonathan, A. E. Lewis, and A. Morris, Mol. Phys. **47**, 1231 (1982).
[4] D. A. Dixon, D. Feller, K. O. Christe *et al.*, J. Am. Chem. Soc. **126**, 834 (2004).
[5] *NIST Chemistry WebBook, NIST Standard Reference Database* Vol. 69, edited by W. G. Mallard and P. J. Linstrom (National Institutes of Standards and Technology, Gaithersburg, MD, 2001) (http://webbook.nist.gov/chemistry).
[6] D. B. Dunkin, F. C. Fehsenfeld, A. L. Schmeltekopf, and E. E. Ferguson, J. Chem. Phys. **54**, 3817 (1971).
[7] D. Smith, N. G. Adams, and T. M. Miller, J. Chem. Phys. **69**, 308 (1978).
[8] W. Lindinger, J. Chem. Phys. **64**, 3720 (1976).
[9] K. Hiraoka, J. Chem. Phys. **91**, 6071 (1989).
[10] S. Matsuoka, H. Nakamura, and T. Tamura, J. Chem. Phys. **75**, 681 (1981).
[11] J. L. McCrumb and P. Warneck, J. Chem. Phys. **66**, 5416 (1977).
[12] S. Matsuoka, H. Nakamura, and T. Tamura, J. Chem. Phys. **79**, 825 (1983).
[13] K. Hiraoka and S. Yamabe, J. Chem. Phys. **90**, 3268 (1989).
[14] A. J. Midey, S. Williams, S. T. Arnold, and A. A. Viggiano, J. Phys. Chem. A **106**, 11726 (2002).
[15] A. A. Viggiano, R. A. Morris, F. Dale, J. F. Paulson, K. Giles, D. Smith, and T. Su, J. Chem. Phys. **93**, 1149 (1990).
[16] P. M. Hierl, J. F. Friedman, T. M. Miller *et al.*, Rev. Sci. Instrum. **67**, 2142 (1996).
[17] S. T. Arnold, S. Williams, I. Dotan, A. J. Midey, R. A. Morris, and A. A. Viggiano, J. Phys. Chem. A **103**, 8421 (1999).
[18] A. J. Midey, S. Williams, S. T. Arnold, I. Dotan, R. A. Morris, and A. A. Viggiano, Int. J. Mass Spectrom. **195**, 327 (2000).
[19] T. H. Dunning, Jr., J. Chem. Phys. **90**, 1007 (1989); R. A. Kendall, T. H. Dunning, Jr., and R. J. Harrison, *ibid.* **96**, 6796 (1992); D. E. Woon and T. H. Dunning, Jr., *ibid.* **98**, 1358 (1993); K. A. Peterson, D. E. Woon, and T. H. Dunning, Jr., *ibid.* **100**, 7410 (1994); A. Wilson, T. van Mourik, and T. H. Dunning, Jr., J. Mol. Struct.: THEOCHEM **388**, 339 (1997).
[20] D. Smith and N. G. Adams, in *Gas Phase Ion Chemistry*, edited by M. T. Bowers (Academic, New York, 1979), Vol. 1, p. 1.
[21] A. A. Viggiano and S. Williams, in *Advances in Gas Phase Ion Chemistry*, edited by N. G. Adams and L. M. Babcock (Academic, New York, 2001), Vol. 4, p. 85.
[22] A. A. Viggiano, W. B. Knighton, S. Williams, S. T. Arnold, A. J. Midey, and I. Dotan, Int. J. Mass Spectrom. **223–224**, 397 (2003).
[23] S. T. Arnold, R. A. Morris, and A. A. Viggiano, J. Chem. Phys. **103**, 9242 (1995); J. V. Seeley, R. A. Morris, A. A. Viggiano, H. Wang, and W. L. Hase, J. Am. Chem. Soc. **119**, 577 (1997).
[24] A. Filippi, A. Troiani, and M. Speranza, J. Phys. Chem. **101**, 9344 (1997).
[25] M. Guilhaus, A. G. Brenton, J. H. Beynon, A. O'Keefe, M. T. Bowers, and J. R. Gilbert, Int. J. Mass Spectrom. **63**, 111 (1985).